Please cite this article in press as: Zhan *et al*., Daurisoline Inhibits Progression of Triple-Negative Breast Cancer by Regulating the γ-Secretase/Notch Axis, Biomol. Ther. (2024), https://doi.org/10.4062/biomolther.2024.131

BIOMOLECULES & THERAPEUTICS

Original Article
Biomol Ther, 1-13 (2024)

Daurisoline Inhibits Progression of Triple-Negative Breast Cancer by Regulating the γ-Secretase/Notch Axis

Xiangyi Zhan[1], Xiaoyong Chen[2], Mei Feng[3], Kuo Yao[3], Kefan Yang[3] and Hui Jia[1,4,*]

[1]*School of Traditional Chinese Medicine, Shenyang Medical College, Shenyang 110034,*
[2]*College of Life Science and Engineering, Northwest Minzu University, Lanzhou 730030,*
[3]*Department of Pathology and Pathophysiology, School of Basic Medical Sciences, Shenyang Medical College, Shenyang 110034,*
[4]*Shenyang Key Laboratory of Vascular Biology, Shenyang 110034, China*

Abstract

Triple-negative breast cancer (TNBC) is a subtype of breast cancer that is challenging to treat and lacks targeted therapeutic drugs in the clinic. Natural active ingredients provide promising opportunities for discovering and developing targeted therapies for TNBC. This study investigated the effects of daurisoline on TNBC and elucidated its potential mechanisms. Using network pharmacology, a correlation was identified between daurisoline, derived from *Menispermum dauricum*, and breast cancer, particularly involving the Notch signaling pathway. The effects of daurisoline on the proliferation, migration, and apoptosis of MDA-MB-231 and MDA-MB-468 cells were evaluated *in vitro*. Additionally, the impact of daurisoline on the growth of MDA-MB-231 xenograft tumors in nude mice was assessed through *in vivo* experiments. Expression levels of Notch signaling pathway-related proteins, including Notch-1, NICD, PSEN-1, Bax, and Bcl-2, were examined using molecular docking and Western blotting to explore the underlying mechanisms of daurisoline's anti-breast cancer effects. It was revealed that daurisoline could effectively inhibit the proliferation and migration of MDA-MB-231 and MDA-MB-468 cells and promote apoptosis. Furthermore, it significantly reduced the growth of subcutaneous tumors in nude mice. Notably, daurisoline could reduce the hydrolytic activity of γ-secretase by binding to the catalytic core PSEN-1, thereby inhibiting activation of the γ-secretase/Notch axis and contributing to its anti-TNBC effects. This study supported the development of naturally targeted drugs for TNBC and provided insights into the research on dibenzylisoquinoline alkaloids, such as daurisoline.

Key Words: Daurisoline, Triple-negative breast cancer, γ-Secretase/Notch axis, Rhizoma menispermi, Dibenzylisoquinoline alkaloid

INTRODUCTION

Breast cancer (BC), the most common malignant tumor with the highest incidence rate among women worldwide, poses a significant threat to patients' physical and mental health (Rugo *et al*., 2021). Triple-negative BC (TNBC) is a particularly concerning subtype. Due to limited targeted therapies, clinical treatment of TNBC primarily relies on traditional methods, such as surgery, radiation, and chemotherapy. Patients with TNBC mainly face poor prognosis, and 40% of patients experience recurrence after surgery. Currently, no frontline treatment exists for this cancer subtype (Malik *et al*., 2022). The screening and development of TNBC-targeted drugs from natural sources present new treatment options (Naeem *et al*., 2021), highlighting the urgent need to explore safe and effective herbal active ingredients for TNBC treatment.

Abnormal activation of the Notch signaling pathway is closely associated with tumor growth, distant metastasis, recurrence, and drug resistance (Zhou *et al*., 2022). Three key proteases are involved in the activation of the Notch signaling pathway: Furin protease, ADAM family proteases, and the γ-secretase complex (Feng *et al*., 2024). Furin protease, located upstream of the Notch signaling pathway, contributes to the maturation of Notch receptors. The ADAM family proteases cleave the Notch receptors, releasing the Notch extracellular domain (NECD). The γ-secretase complex, a large transmembrane protein complex, performs the final cleavage of the Notch receptors in the intracellular domain. Following cleavage by γ-secretase, the Notch intracellular domain (NICD) is released, translocates to the nucleus, and binds to CSL (CBF1

Open Access **https://doi.org/10.4062/biomolther.2024.131**

Received Aug 6, 2024 **Revised** Sep 13, 2024 **Accepted** Nov 14, 2024
Published Online 000 1, 2024

***Corresponding Author**
E-mail: huijia412413@symc.edu.cn
Tel: +86-024-62215837, Fax: +86-024-62215837

in humans, suppressor of Hairless in *Drosophila*, and LAG in *C. elegans*), initiating the transcription of downstream genes (Kopan and Ilagan, 2009).

The γ-secretase complex consists of five subunits: the homologous proteins presenilin-1 (PSEN-1) and presenilin-2 (PSEN-2), along with nicastrin (NCSTN), anterior pharynx-defective 1 (APH-1), and presenilin enhancer-2 (PEN-2). Nicastrin (NCSTN) is a transmembrane glycoprotein that plays a pivotal role in the intramembrane proteolysis of integral membrane proteins, including Notch receptors and amyloid precursor protein-β, in the γ-secretase complex (Jia *et al*., 2021c). In γ-secretase, PSEN-1 serves as a key regulatory factor in the crosstalk between Notch and Wnt signaling pathways, contributing to cleavage site execution and substrate recognition (Serneels *et al*., 2023). Loss of PSEN-1 activity significantly impacts γ-secretase function.

Rhizoma Menispermi (RM, *Menispermum dauricum* DC.) is the rhizome of *Menispermum dauricum* in the Menispermaceae family. It is known for its effects of clearing heat and detoxifying, reducing swelling and pharyngitis, dispelling wind, and relieving pain. Bisbenzylisoquinoline alkaloids are a unique component found in RM. By substituting active groups, such as -OH, -OCH_3, and -CH_3 at different positions on the structural nucleus, various compounds are derived, including dauricine, daurisoline, daurinoline, dauricinoline, dauriciline, dauricoline, and dauricicoline. These compounds have been isolated and purified from RM, and their structures have been elucidated (Fig. 1). Preliminary research has assessed screening the activity of a series of bisbenzylisoquinoline alkaloid compounds. Among them, daurisoline has been identified as a representative compound with significant anti-TNBC activity. This study concentrated on the therapeutic potential of daurisoline against MDA-MB-231 (TNBC cell line) and MDA-MB-468 cells (another TNBC cell line). Additionally, the inhibitory effects of daurisoline on the proliferation, invasion, and migration of TNBC cells were examined both *in vitro* and *in vivo*.

MATERIALS AND METHODS

Agents and cell culture

Daurisoline (CAS: 2189-80-2, purity ≥95%; Purify Co., Ltd., Chengdu, China), doxorubicin (CAS: 23214-92-8, purity ≥97%; Selleck Co., Ltd.,, Shanghai, China), sulfonylrhodamine B assay kit (Abcam, Cambridge, UK), crystal violet staining solution (Beyotime, Shanghai, China), LDH assay kit (Beyotime), Hoechst 33342 staining solution for live cells (Beyotime), cell cycle and apoptosis analysis kit (Beyotime), annexin V-FITC apoptosis detection kit (Beyotime), Matrigel basement membrane matrix (Solarbio Science & Technology Co., Ltd., Beijing, China), 11-245KD color mixed protein marker (Solarbio Science & Technology Co., Ltd.), NICD (Val1744) (D3B8) rabbit mAb #4147 (Cell Signaling Technology (CST), Waltham, MA, USA), Notch-1 (D1E11) XP® rabbit mAb #3608 (CST), GAPDH (D16H11) XP® rabbit mAb #8884 (CST), Bax (Wanleibio Co., Ltd., Shenyang, China), Bcl-2 (Wanleibio), presenilin 1 (D39D1) rabbit mAb #5643 (CST), and electrochemiluminescence (ECL) detection kit (Wanleibio) were uti-

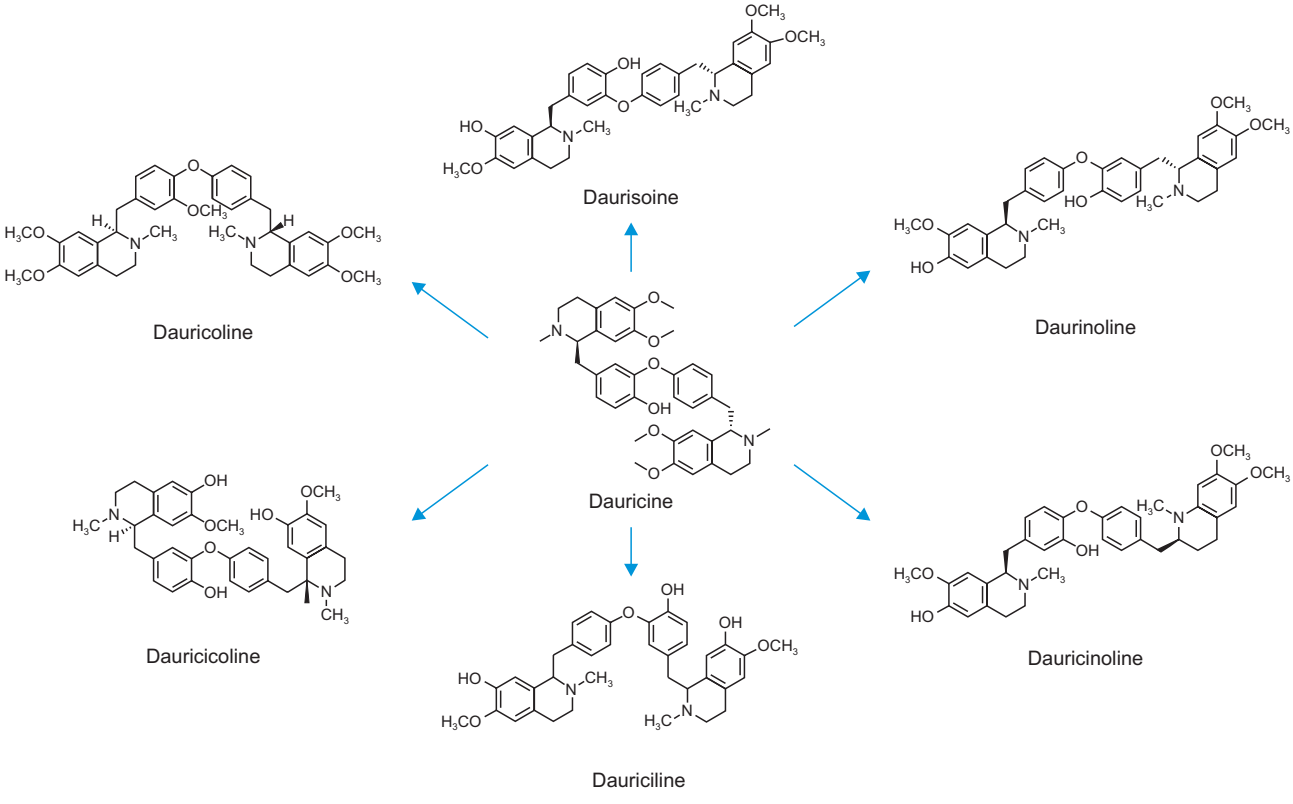

Fig. 1. Representation of bisbenzylisoquinoline alkaloids by daurisoline. By modifying the bisbenzylisoquinoline structure with substitutions of -CH_3, -OH, and -OCH_3 groups at various positions, a series of active compounds are generated.

lized in this study.

Human BC cell lines (MDA-MB-231 and MDA-MB-468) were purchased from the American Type Culture Collection (ATCC; Manassas, VA, USA) in June 2022. The cell lines were authenticated by STR analysis, and the most recent validation was completed in March 2023. Cells were cultured in a high-glucose Dulbecco's modified Eagle's medium (DMEM) supplemented with 1% penicillin-streptomycin and 10% fetal bovine serum (FBS) and maintained at 37°C in a humidified atmosphere containing 5% CO_2. The cell lines were passaged three times before being utilized for *in vitro* experiments.

Anti-proliferation assessment

The effect of daurisoline on the viability of human BC cells was investigated using the sulforhodamine B (SRB) colorimetric assay (Jia *et al*., 2021b). MDA-MB-231 and MDA-MB-468 cells in the logarithmic growth phase were collected and seeded into 96-well plates at appropriate densities. After the cells adhered, they were incubated with daurisoline (1-50 μM) for 24, 48, and 72 h. The cells were thereafter fixed with 50% trichloroacetic acid solution, stained with 0.4% SRB, and the optical density (OD) value was measured at 540 nm using a microplate reader.

The effect of daurisoline on the proliferation of human BC cells at low density was figured out using plate cloning assay (Jia *et al*., 2021b). The cells were seeded into 6-well plates at an appropriate density and incubated with daurisoline (6.25, 12.5, and 25 μM) and doxorubicin (1 μM) for 48 h. Subsequently, the medium was changed, and the culture was continued for 11 days. Cell colonies were stained with 0.1% crystal violet, and photographs were taken. The dye was dissolved in 30% glacial acetic acid and then transferred to a 96-well plate. The OD value was measured at 570 nm using a microplate reader.

The effect of daurisoline on the cell cycle of human BC cells was assessed using propidium iodide (PI) staining (Jia *et al*., 2021a). Cells were seeded into 6-well plates at an appropriate density and incubated with daurisoline (6.25, 12.5, and 25 μM) and doxorubicin (1 μM) for 48 h. The cells were processed according to the instructions of the cell cycle assay kit, stained with PI, and analyzed by flow cytometry (FCM). After data collection, the FlowJo software (https://www.flowjo.com/) was utilized to analyze the cell cycle. All experiments were conducted in parallel three times, and the data were statistically analyzed.

Pro-apoptosis assessment

Daurisoline-induced late apoptosis of human BC cells was determined using lactate dehydrogenase (LDH) assay (Jia *et al*., 2021b). The cells were incubated with different concentrations of daurisoline (6.25, 12.5, and 25 μM) and doxorubicin (1 μM) for 48 h. The concentration of lactate dehydrogenase in the cell supernatant was measured using a microplate reader according to the instructions provided by the LDH kit's manufacturer.

Hoechst 33342 staining was performed to assess the ability of daurisoline to induce apoptosis in BC cells (Jia *et al*., 2021a). The cells were incubated with daurisoline (6.25, 12.5, and 25 μM) and doxorubicin (1 μM) for 48 h, followed by incubation with Hoechst 33342 fluorescent dye for 40 min. After staining, the cells were thrice washed with phosphate-buffered saline (PBS) solution, and images were taken using a fluorescence microscope.

The early and late apoptosis of human BC cells treated with daurisoline was investigated using Annexin V-FITC/PI (AV/PI) staining (Jia *et al*., 2021b). The cells were incubated with daurisoline (6.25, 12.5, and 25 μM) and doxorubicin (1 μM) for 48 h, and then fixed overnight with 70% ethanol. Following the instructions of the AV/PI apoptosis kit, the samples were stained in the dark for 30 min and analyzed by FCM. All experiments were performed in parallel three times, and the data were statistically analyzed.

Migration and invasion assays

The effect of daurisoline on the migration of human BC cells was assessed using wound-healing assay (Jia *et al*., 2021b). Cells in the logarithmic growth phase were harvested and seeded into 6-well plates, where they formed confluent monolayers. A 200 μL pipette tip was utilized to gently scratch the confluent surface of the cells, after which the scratched cells were washed with PBS solution. The cells were subsequently incubated with different concentrations of daurisoline (6.25, 12.5, and 25 μM) and doxorubicin (1 μM) for 48 h. Images were taken at 0 and 48 h using an inverted microscope, and the migration effect was evaluated by measuring the degree of healing in the scratched area.

The effect of daurisoline on the invasion of human BC cells was evaluated using transwell assay (Jia *et al*., 2021b). Matrigel was applied to the upper chamber of a transwell plate and allowed to solidify overnight. The following day, cells were seeded onto the gelled surface of the upper chamber and incubated with different concentrations of daurisoline (6.25, 12.5, and 25 μM) and doxorubicin (1 μM). Complete medium containing 10% FBS was added to the lower chamber. After 48 h of treatment, the cells that had invaded through the membrane to the lower side were stained with 0.1% crystal violet, observed with an inverted microscope, and photographed. All experiments were performed in parallel three times, and the data were statistically analyzed.

In vivo experiment

The *in vivo* therapeutic effects of daurisoline on BC cells were examined using a nude mouse xenograft model (Jia *et al*., 2021a). BALB/c nude Crlj mice (weight, 16-20 g; 6-week-old; female) were obtained from Vital River Laboratory Animal Technology Co., Ltd. (Beijing, China). A single-cell suspension of MDA-MB-231 was subcutaneously inoculated into the scapular region of nude mice until the volume of the subcutaneous tumor reached 100-150 mm^2. Mice meeting the inclusion criteria were divided into four groups (four mice per group) using a balanced random grouping method. Daurisoline (1 and 5 mg/kg) was intraperitoneally injected every two days, while doxorubicin (1 mg/kg) was administered orally for 14 days. After the treatment, all animals were euthanized using 3% isoflurane inhalation anesthesia for 2-3 min. Organs and tumor tissues were collected and stored at –80°C for subsequent experiments. The experimental protocols were conducted in accordance with the ARRIVE guidelines, and the study protocol was approved by the Animal Ethics Committee of Shenyang Medical College (Shenyang, China; Approval No. SYYXY2023101901).

Molecular docking and determination of the expression levels of key proteins in the Notch signaling pathway

Daurisoline was docked into the active site of γ-secretase (PDB code: 7C9I) using the Glide module of Schrödinger Maestro 2018. The three-dimensional structure of daurisoline was generated with Chem-Bio-Draw Ultra 13.0 software (https://www.scientific-computing.com/press-releases/chembiooffice-ultra-130-suite). The ligand and protein were prepared using the LigPrep module and the Protein Preparation Wizard module of Schrödinger Maestro 2018 (https://www.schrodinger.com/platform/products/ligprep/, https://www.schrodinger.com/life-science/learn/white-papers/protein-preparation-wizard/), respectively. Additionally, receptor grids for molecular docking were generated using the Receptor Grid Generation tool, and other docking parameters were set to their default values.

The effect of daurisoline on the expression levels of key factors in the Notch signaling pathway was examined *in vivo* using Western blotting. The protein content extracted from tumor tissue samples was determined by the bicinchoninic acid (BCA) protein quantification method. Western blot analysis was performed according to the established protocols, and the blots were visualized using an enhanced chemiluminescence (ECL) detection kit and the ChemiDoc™ imaging system (Bio-Rad Laboratories, Hercules, CA, USA). Image processing was conducted using ImageJ software (https://imagej.affinitycn.cn/?bd_vid=8016646872135780194#header).

Statistical analysis

All data were presented as the mean ± standard deviation (SD) from at least three biological replicates. Statistical differences between two groups were compared using unpaired t-test through GraphPad Prism 7.0 software (GraphPad Software Inc., San Diego, CA, USA). A P-value of less than 0.05, 0.01, 0.001, and 1×10^{-4} was considered statistically significant and marked as "*", "**", "***", and "****," respectively.

RESULTS

Screening and identification of daurisoline as a γ-secretase inhibitor

Chemical constituents and related targets of RM were collected from the traditional Chinese medicine system (TCMSP) database to construct a relationship network. The results of the landscape pharmacology network and the selection of hub genes are presented in Fig. 2A. Cytoscape 3.10.2 software (https://cytoscape.org/) was utilized to visualize the network of ingredient-target relationships, identifying 13 active ingredients and 94 related targets. Among them, daurisoline, a unique compound found in RM, received particular attention.

Next, the active ingredient-related targets of RM were intersected with BC-related targets using Venn analysis. As illustrated in Fig. 2B, the predicted candidate targets of RM overlapped with BC-related targets, resulting in a total of 17 intersected targets (excluding duplicates). A protein-protein interaction (PPI) network analysis was conducted for the intersecting targets of RM and BC, which targets with scores greater than 0.7 were selected to construct a PPI network using the STRING database. This network consisted of 13 nodes and 50 edges, with an average node degree of 7.25 and an average local clustering coefficient of 0.78 (Fig. 2C). BCL2, NOTCH1, and CASP3 exhibited high connectivity, functioning as central hubs in the PPI network.

Disease-related enrichment analysis of RM genes was performed using Gene Ontology (GO) chord plots (Log fold-change (FC) values >1 or <–1). The results indicated that BC ranked second, suggesting that RM-related genes could be involved in BC treatment (Fig. 2D). Subsequently, the Kyoto Encyclopedia of Genes and Genomes (KEGG) pathway enrichment analysis was conducted on the relevant targets of RM's active ingredients, identifying the top 17 enriched KEGG pathways ($p<0.05$). As displayed in Fig. 2E, the regulation of active ingredient-related targets in RM was predominantly associated with the Notch signaling pathway, indicating that daurisoline could influence BC through the γ-secretase/Notch axis.

Daurisoline inhibited the proliferation of TNBC cells

To investigate the inhibitory effect of daurisoline on TNBC cell proliferation, MDA-MB-231 and MDA-MB-468 cells were treated with different concentrations of daurisoline (3.125-100 μM) for 24, 48, and 72 h, respectively. The proliferation of TNBC cells was assessed using the sulforhodamine B (SRB) assay. As illustrated in Fig. 3A, 3B, daurisoline significantly inhibited the proliferation of TNBC cells, and the inhibitory activity demonstrated dependence on both time and concentration. The half-maximal inhibitory concentration (IC_{50}) values for daurisoline treatment of MDA-MB-231 and MDA-MB-468 cells after 48 h were 18.31 ± 1.58 and 16.25 ± 1.22 μM, respectively.

Additionally, the cytotoxicity of daurisoline on normal breast cells, MCF-10A, was examined. The results indicated that when the concentration of daurisoline was elevated to 200 μM, the inhibition rate on MCF-10A cells was only about 20% (Fig. 3C). This suggests that daurisoline, as a natural active ingredient, exhibits selectivity towards TNBC cells while demonstrating low toxicity to normal breast cells.

The long-term inhibitory effect of daurisoline on both types of TNBC cells under very low-density conditions was evaluated using the cell colony formation assay. The results revealed that daurisoline (6.25, 12.5, and 25 μM) effectively inhibited colony formation of MDA-MB-231 and MDA-MB-468 cells compared with the control group (Fig. 3D), with statistically significant findings (Fig. 3E, 3F). Doxorubicin served as a positive control in this study, as it is the preferred drug for the clinical treatment of TNBC and has demonstrated notable inhibitory activity on MDA-MB-231 cells. These data suggested that daurisoline could effectively inhibit the proliferation of TNBC cells.

The effect of daurisoline on the TNBC cell cycle was analyzed through PI staining combined with FCM. As illustrated in Fig. 3G, compared with the control group, TNBC cells exhibited significant arrest in the S phase following treatment with daurisoline (6.25 μM). As a positive control, doxorubicin (1 μM) was used to treat MDA-MB-231 and MDA-MB-468 cells for 48 h, resulting in cell cycle arrest in the G2/M phase. It is noteworthy that cetuximab was used as an irrelevant control in the cell cycle assay. The findings indicated that daurisoline could inhibit cell proliferation by inducing S phase arrest in TNBC cells, with statistically significant results (Fig. 3H, 3I).

Daurisoline induced apoptosis in TNBC cells

During the investigation of daurisoline's effect on inhibiting TNBC cell proliferation, its ability to promote apoptosis was

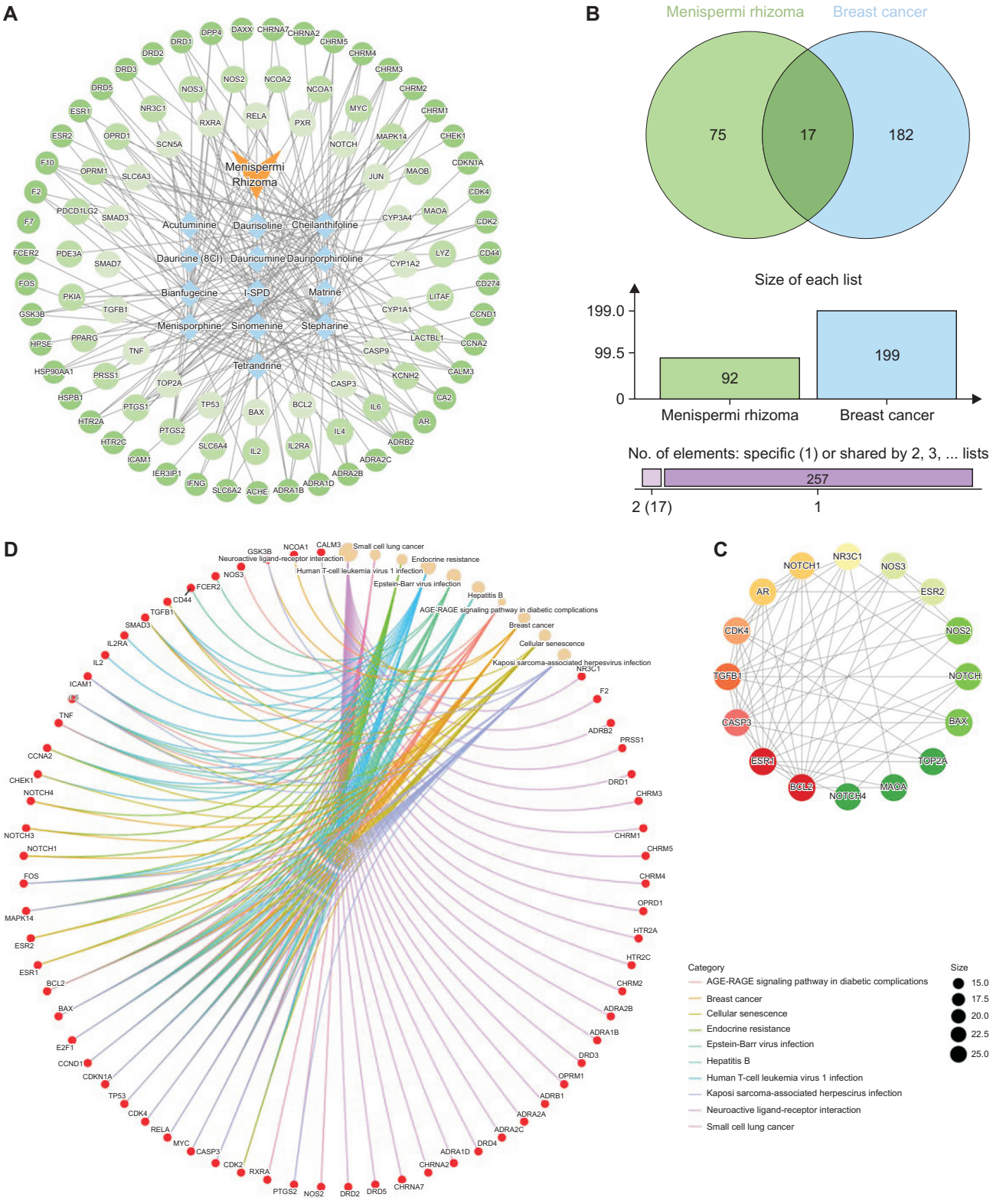

Fig. 2. Active ingredients and key targets of RM in inhibiting the progression of BC. (A) The network of RM: active ingredients and targets. Interaction between active components and drug targets of RM. The orange triangle represents RM, the blue squares represent the active ingredients of RM, and the green circles represent the potential drug targets of the active ingredients. (B) Venn diagram. A Venn diagram shows the intersection between RM (drug gene) and BC (disease gene). The 17 overlapping targets represent the candidate targets of RM against BC. (C) Protein-protein interaction network. Illustrating the intersection targets of RM. (D) GO enrichment analysis. Analysis of the key genes in RM, with an emphasis on breast cancer as the candidate disease. (E) Results of the KEGG pathway enrichment analysis (Top 17). For interpretation of color references in this figure legend, please refer to the online version of this article.

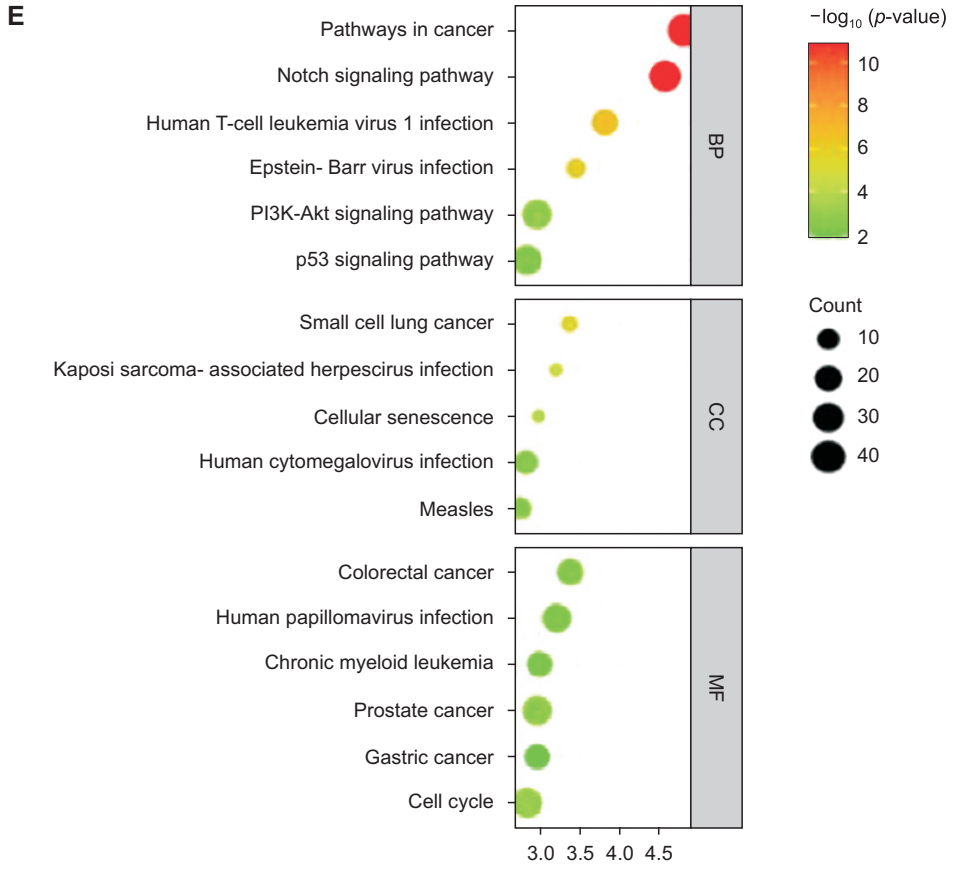

Fig. 2. Continued.

also explored. This effect was evaluated through cell morphology observation, AV/PI double staining combined with FCM, and LDH release assay. The results of Hoechst 33342 staining indicated that, compared with the control group, MDA-MB-231 and MDA-MB-468 cells treated with different concentrations of daurisoline for 48 h exhibited an increase in the number of apoptotic cells and the formation of apoptotic bodies. As the concentration of daurisoline increased, the number of viable cells significantly decreased (Fig. 4A).

To verify the morphological observations, LDH release assay was conducted. LDH is a cytoplasmic enzyme that is released into the culture medium when the cell membrane is compromised, indicating late apoptosis. The results demonstrated that after treating MDA-MB-231 and MDA-MB-468 cells with daurisoline for 48 h, LDH concentration in the cell culture medium significantly increased compared with the control group, comprising statistically significant results (Fig. 4B, 4C).

AV/PI double staining was employed to detect early and late apoptosis in MDA-MB-231 and MDA-MB-468 cells following daurisoline treatment. The findings indicated that, compared with the control group, the proportion of viable cells gradually decreased while that of early apoptotic cells significantly increased following 48 h of daurisoline treatment (Fig. 4D), with statistically significant results (Fig. 4E, 4F). Overall, the findings demonstrated that daurisoline could effectively promote apoptosis in TNBC cells.

Daurisoline blocked the migration and invasion of TNBC cells

Metastasis and infiltration are the main reasons for treatment failure in cancer patients. The wound healing assay was employed to evaluate the effect of daurisoline on the metastatic abilities of MDA-MB-231 and MDA-MB-468 cells. The results of wound healing assay revealed that, compared with the control group, increasing concentrations of daurisoline effectively reduced the metastatic ability of MDA-MB-231 and MDA-MB-468 cells after 48 h. As a natural compound, daurisoline exhibited an anti-metastatic effect at 6.25 μM, which is comparable to the effect of the first-line chemotherapy drug doxorubicin at 1 μM (Fig. 5A), accompanying by statistically significant results (Fig. 5B, 5C).

Transwell assay was employed to evaluate the effects of daurisoline on the migration and invasion abilities of MDA-MB-231 and MDA-MB-468 cells. In this experiment, Matrigel was added to the upper layer of the membrane in the Transwell chamber to assess invasion. After treatment with daurisoline (12.5 μM), the invasion and migration abilities of MDA-MB-231 and MDA-MB-468 cells were gradually reduced, and the number of TNBC cells crossing the Matrigel significantly decreased, as displayed in Fig. 5D, accompanying by statistically significant results (Fig. 5E-5H). The Transwell assay data not only confirmed that daurisoline could effectively inhibit the migration and invasion of TNBC cells, but also validated the results of the wound healing experiment.

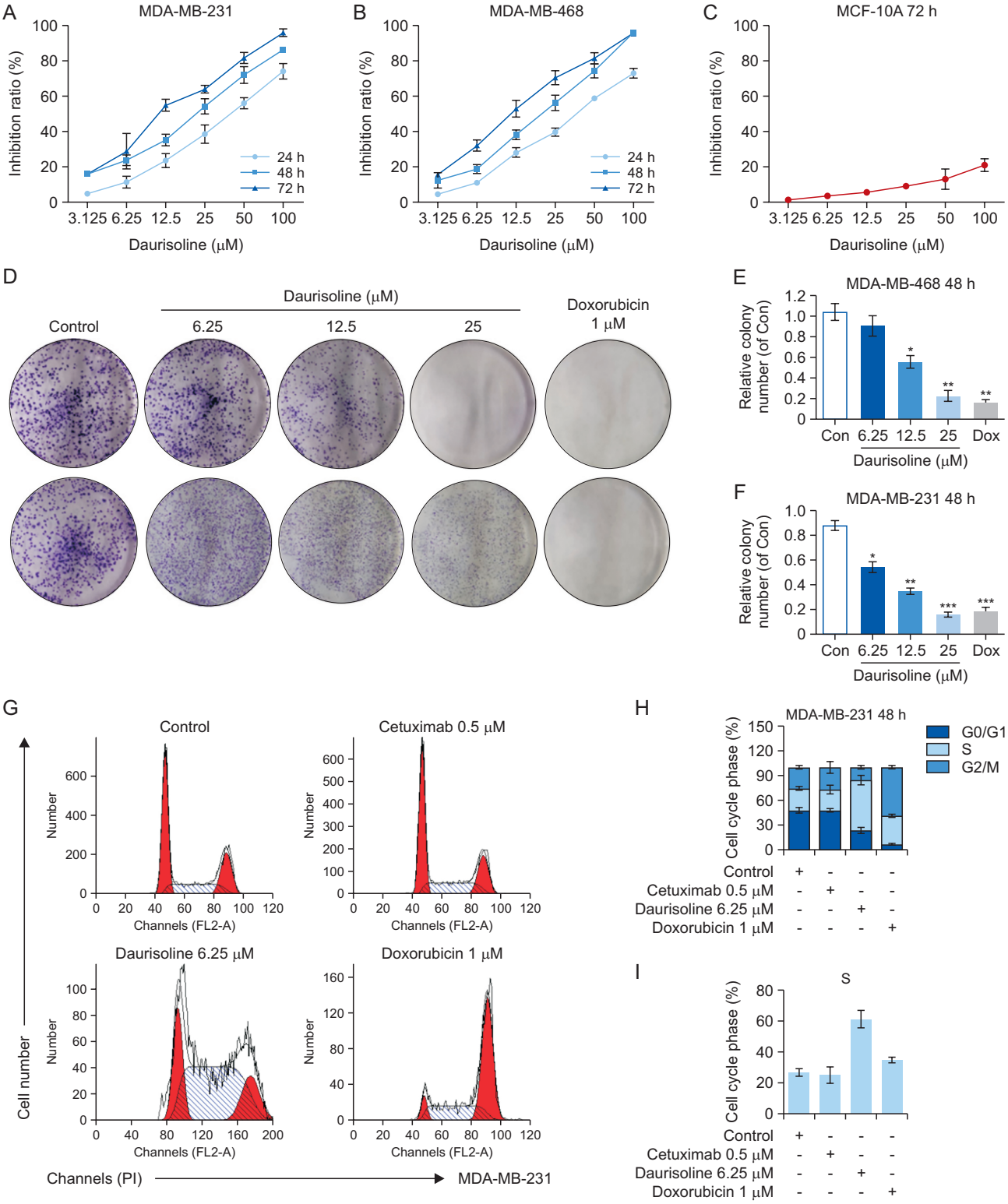

Fig. 3. Daurisoline inhibits the proliferation of MDA-MB-231 and MDA-MB-468 cells. (A, B) The effects of daurisoline on MDA-MB-231 and MDA-MB-468 cell viability were evaluated by SRB assay, and the inhibition rate exhibited a certain concentration-time dependence. (C) The cytotoxicity of daurisoline on human normal breast MCF-10A cells was investigated by SRB. (D) The effect of daurisoline/doxorubicin on the colony-forming ability of MDA-MB-231 and MDA-MB-468 cells for 48 h was evaluated by colony formation assay. (E, F) Quantitative histograms of colony formation results for two TNBC lines. Each value is presented as the mean (±SEM) from triplicate samples. *p<0.05, **p<0.01, ***p<0.001 *versus* control group. (G) FACS analysis of the cell cycle distribution after treatment with daurisoline/doxorubicin for 48 h in the MDA-MB-231 and MDA-MB-468 cells. (H, I) Quantitative histogram of the G1, S, and G2/M phases of MDA-MB-231 cell cycle. Each value is presented as the mean (±SD) from triplicate samples.

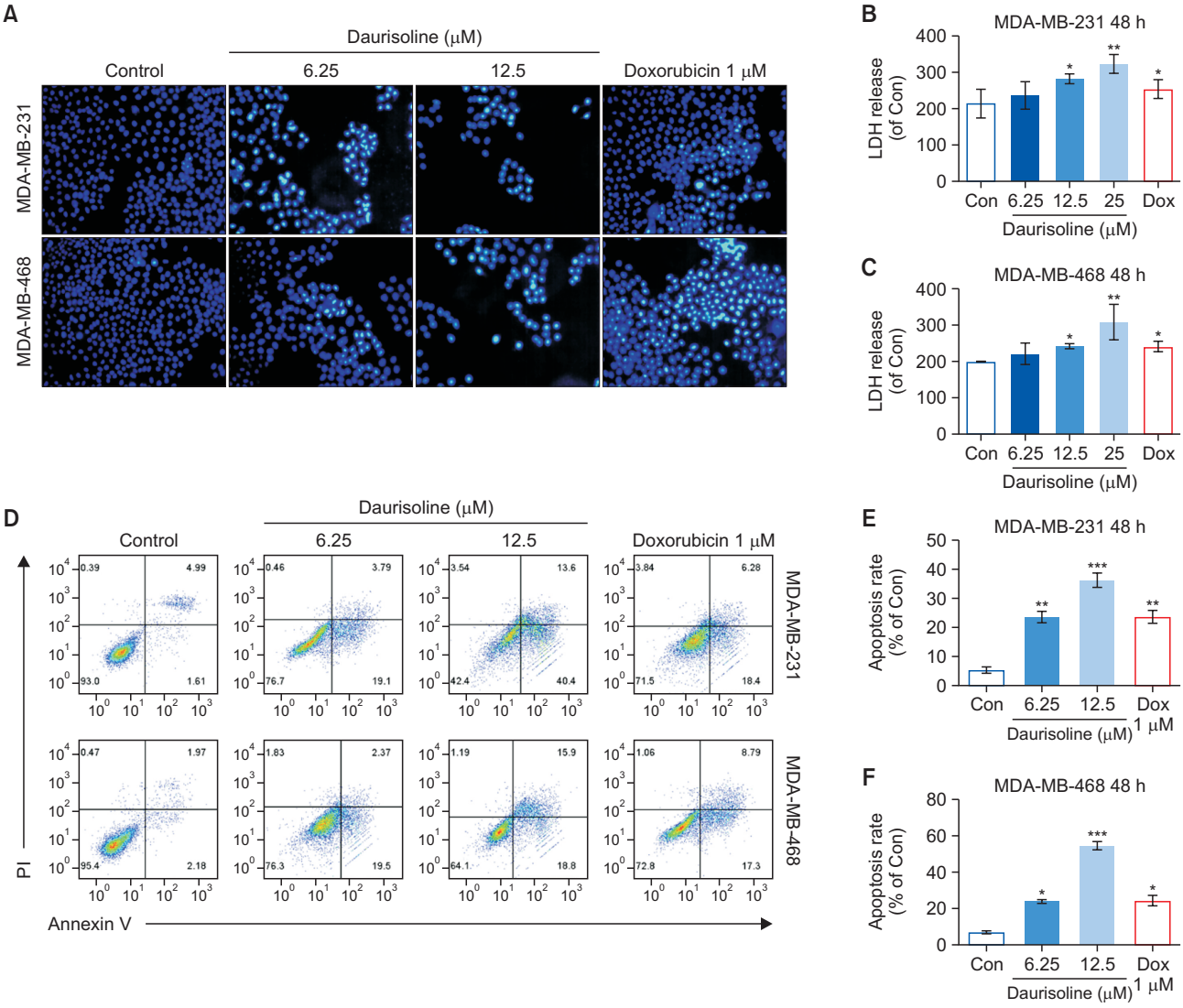

Fig. 4. Daurisoline promotes apoptosis of MDA-MB-231 and MDA-MB-468 cells. (A) The apoptosis of MDA-MB-231 and MDA-MB-468 cells after Daurisoline/Doxorubicin treatment was assessed using Hoechst 33342 staining (scale bar=100 μm, ×200 magnification). (B, C) The percentage of LDH released from MDA-MB-231 and MDA-MB-468 cells after treatment with daurisoline or doxorubicin. (D) The ratio of early and late apoptosis in MDA-MB-231 and MDA-MB-468 cells was assessed using Annexin V-FITC/PI (AV/PI) double staining. (E, F) Quantitative histograms of AV/PI double-staining results for the two TNBC cell lines. Each value is presented as the mean (±SEM) from triplicate samples. **p*<0.05, ***p*<0.01, ****p*<0.001 *versus* control group.

Daurisoline inhibited the growth of human TNBC xenograft tumors

A TNBC nude mouse xenograft model was established to evaluate the therapeutic effect of daurisoline on TNBC *in vivo*. Daurisoline (1 and 5 mg/kg) and doxorubicin (1 mg/kg) were administered intragastrically daily for 14 days (Fig. 6A). During the treatment, the diet and water intake of experimental animals were monitored, and the volume of subcutaneous tumors and the body weight of animals were measured regularly. At the end of the treatment, the experimental animals were anesthetized using 3% isoflurane, euthanized uniformly, and tumor and organ tissues were collected (Fig. 6B).

Histological data indicated that the untreated group had significant cancer nests, with notable destruction of tissue structure. In comparison, daurisoline effectively reduced the formation of cancer nests and significantly restored normal tissue structure (Fig. 6C). Daurisoline (5 mg/kg) significantly inhibited the growth of subcutaneous tumors in MDA-MB-231 cells, accompanied by statistically significant results (p<0.05, Fig. 6D, 6E).

During the *in vivo* assessment of daurisoline's antitumor efficacy, changes in the body weight of experimental animals were also monitored throughout daurisoline administration. Throughout the treatment period, the body weight of nude mice in the untreated group exhibited a downward trend, while the body weight of animals in the daurisoline and doxorubicin treatment groups increased to varying degrees (Fig. 6F). These findings suggest that daurisoline can maintain the appetite of experimental animals while inhibiting TNBC growth. Based on the subcutaneous tumor volume data collected *in*

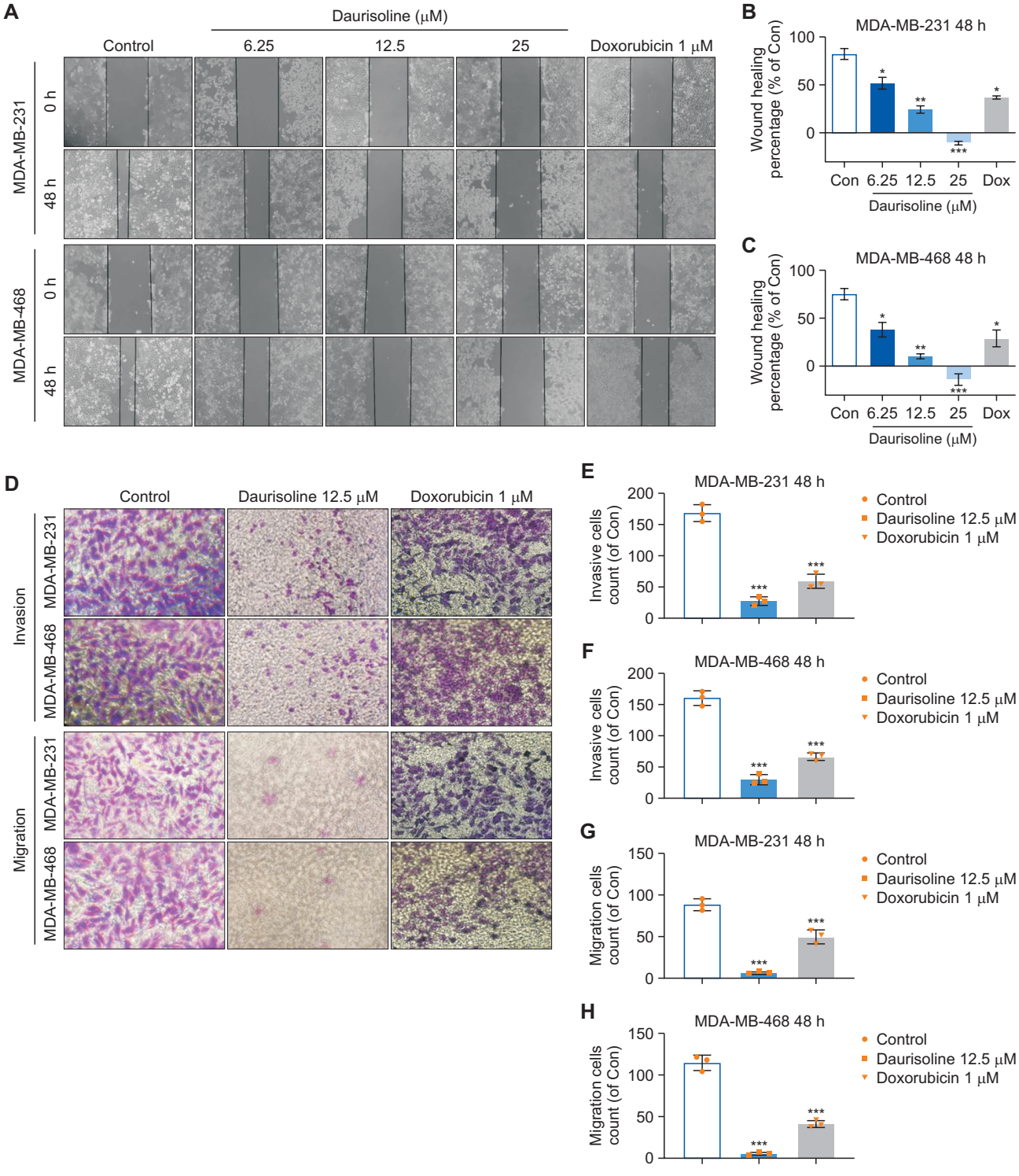

Fig. 5. Daurisoline inhibits migration and invasion of MDA-MB-231 and MDA-MB-468 cells. (A) After 48 h of daurisoline/doxorubicin treatment, the effect on the migration ability of TNBC cells was evaluated by wound healing assay. (B, C) Quantitative histograms of wound healing assay results for TNBC cell lines. (D) After 48 h of daurisoline/doxorubicin treatment, the effect on the invasion and migration abilities of TNBC cells was evaluated by Transwell assay. (E, F) Quantitative histograms of invasion assay results for TNBC cell lines. (G, H) Quantitative histograms of migration assay results for TNBC cell lines. Each value is presented as the mean (±SEM) from triplicate samples. *p<0.05, **p<0.01, ***p<0.001 *versus* control group.

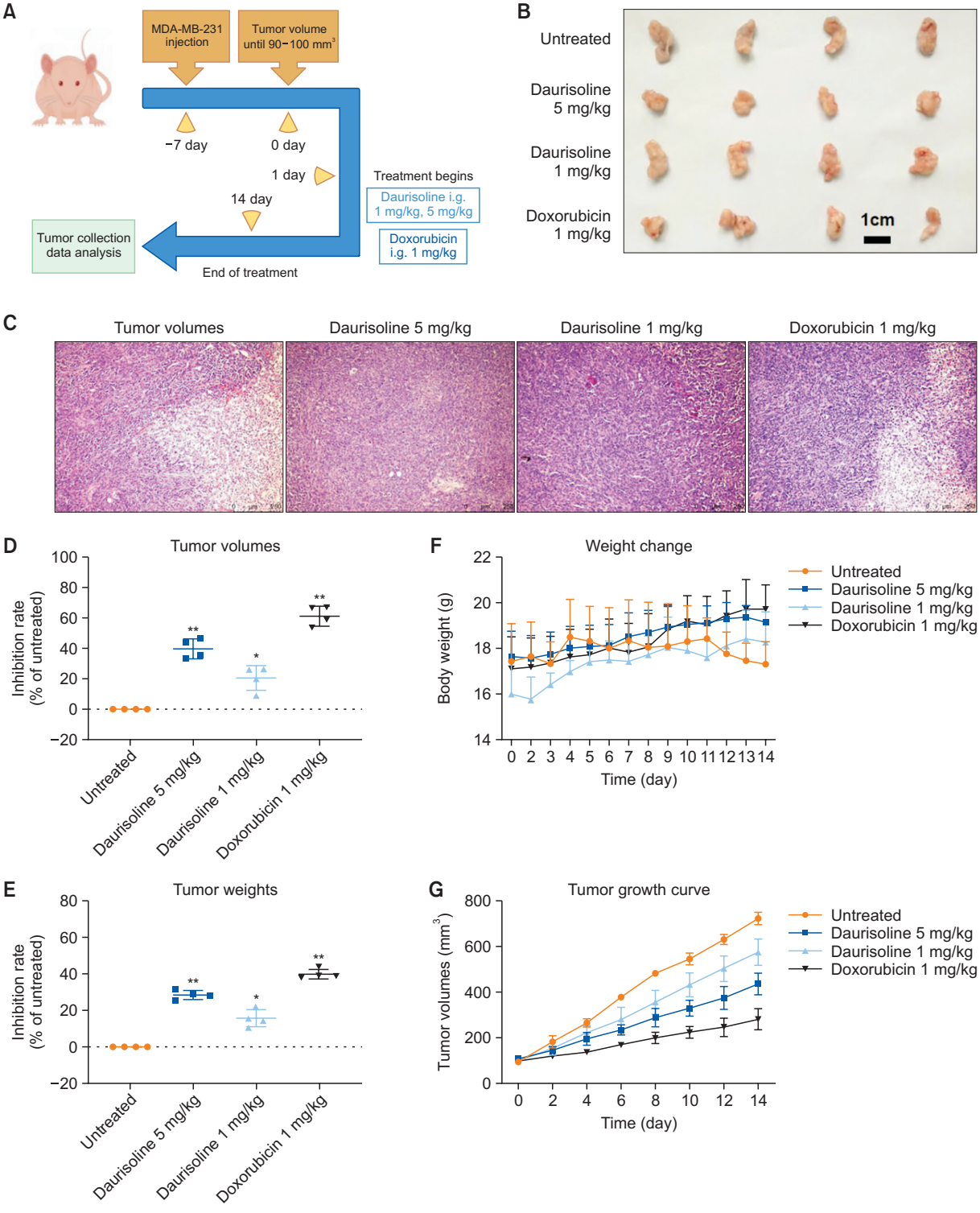

Fig. 6. Daurisoline inhibits the growth of xenograft subcutaneous tumors in MDA-MB-231 cells. (A) Establishment of a nude mouse xenograft model and treatment plan. (B) The photo collection of xenograft subcutaneous tumors in nude mice. (C) The tumor tissues of xenograft mice were histologically analyzed by HE staining (scale bar=250 μm). (D) A quantitative histogram of tumor inhibition rate was analyzed by the volume of subcutaneous tumors (n=4). (E) A quantitative histogram of tumor inhibition rate was analyzed by the weight of the subcutaneous tumors (n=4). (F) The weight change of nude mice during 14 days of daurisoline/doxorubicin treatment. (G) Graph displaying the changes in the volume of xenograft tumors in various groups of animals during treatment. Each value is presented as the mean (±SEM) from triplicate samples. **p*<0.05, ***p*<0.01 *versus* control group.

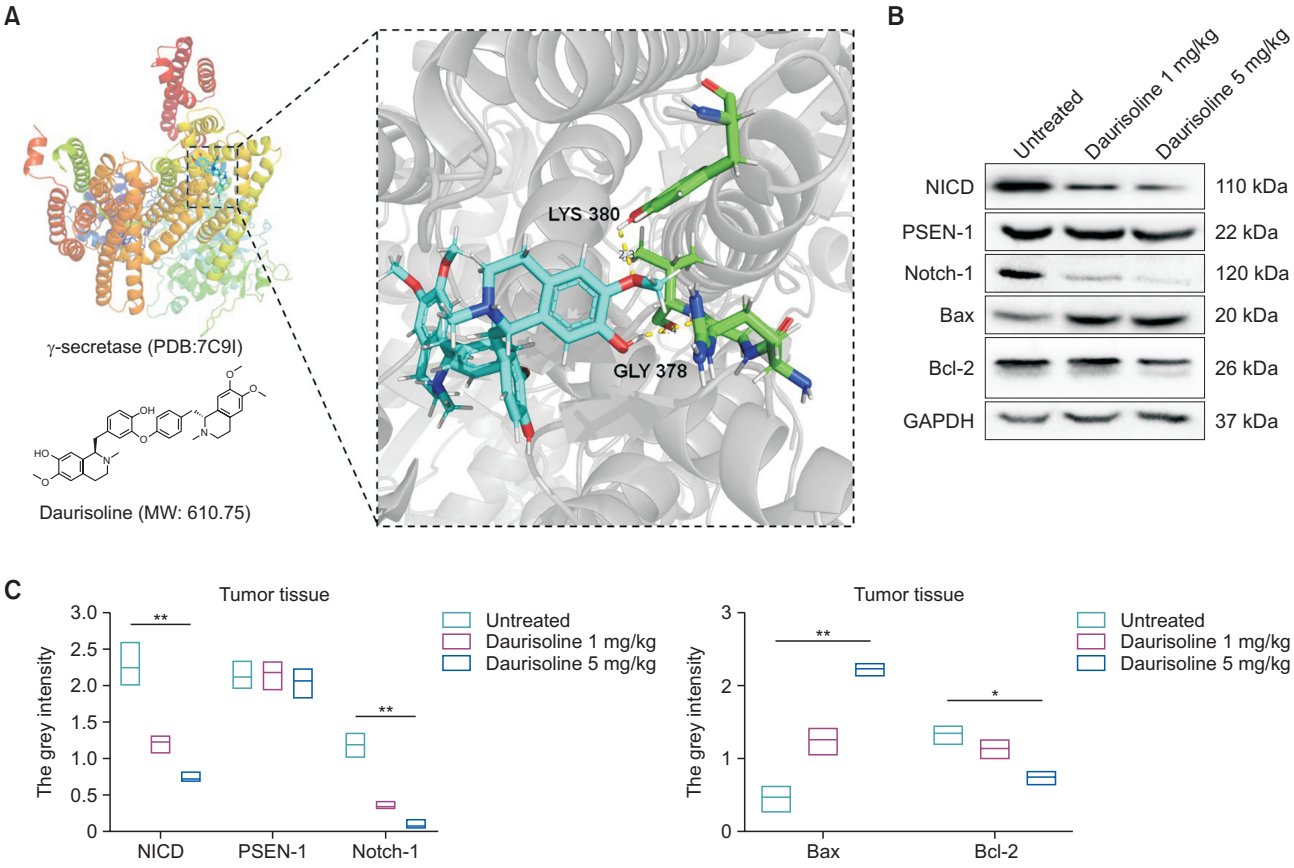

Fig. 7. Daurisoline inhibits TNBC growth via regulating the γ-secretase/Notch axis. (A) Molecular docking of the interaction between γ-secretase (PDB: 7C9I) and daurisoline, exhibiting the protein active site of PSEN-1. The yellow dotted lines indicate hydrogen bonds formed with hydroxyl groups. (B) Western blotting was utilized to detect changes in the expression levels of the Notch intracellular domain (NICD), the γ-secretase catalytic core PSEN-1, the Notch-1 receptor, and the apoptosis-indicating proteins Bax and Bcl-2 in tumor tissue after daurisoline treatment. (C) Statistical analysis of the Western blotting results. Each value is presented as the mean (±SEM) from triplicate samples. *p<0.05, **p<0.01 versus control group.

vivo, a tumor growth curve was plotted. As daurisoline treatment progressed, the growth rate of subcutaneous tumors in nude mice gradually decreased, indicating that daurisoline could effectively inhibit tumor growth, as illustrated in Fig. 6G.

Daurisoline inhibited BC cell growth by the γ-secretase/Notch axis

After confirming the *in vivo* effects of daurisoline on BC, preliminary exploration of its mechanism was conducted. To further evaluate the effect of daurisoline on the Notch signaling pathway, the possible binding mode of daurisoline to γ-secretase (PDB code: 7C9I) was predicted using molecular docking (Fig. 7A). It was revealed that the hydroxyl group on daurisoline could form two key hydrogen bonds with LYS380 and GLY378 in PSEN-1 (the catalytic core of γ-secretase). Importantly, daurisoline exhibited a strong affinity for the active center of γ-secretase.

To further confirm the function of daurisoline through the Notch signaling pathway, Western blotting was employed to detect the expression levels of the Notch intracellular domain (NICD), the γ-secretase catalytic core PSEN-1, the Notch-1 receptor, and apoptosis-indicating proteins (Bax and Bcl-2) in tumor tissue following daurisoline treatment. As displayed in Fig. 7B, 7C, after 14 days of treatment, the protein expression level of PSEN-1 did not significantly vary, while the level of NICD was significantly reduced, confirming a reduction in the hydrolytic activity of γ-secretase. Moreover, the protein expression level of Notch-1 was significantly downregulated, indicating that activation of the Notch signaling pathway was blocked. Additionally, Bax and Bcl-2 are important indicators of cell apoptosis. They regulate apoptosis by forming homodimers or heterodimers. An increase in Bax expression level and a decrease in Bcl-2 expression level induce apoptosis by promoting homodimer formation.

PSEN-1 is a key subunit of the γ-secretase complex and the catalytic core for its hydrolytic function. The results indicated that treatment with daurisoline resulted in decreased expression levels of Notch-1 receptors and NICD, confirming that the hydrolytic activity of γ-secretase was affected and the activation of the Notch signaling pathway was blocked. The changes in Bax and Bcl-2 expression levels further indicated apoptosis in TNBC cells. Notably, the protein level of PSEN-1 remained unchanged, suggesting that while daurisoline inhibited PSEN-1's catalytic activity by binding to its active site, it did not alter the overall expression level of PSEN-1.

Therefore, it is speculated that daurisoline, as a natural

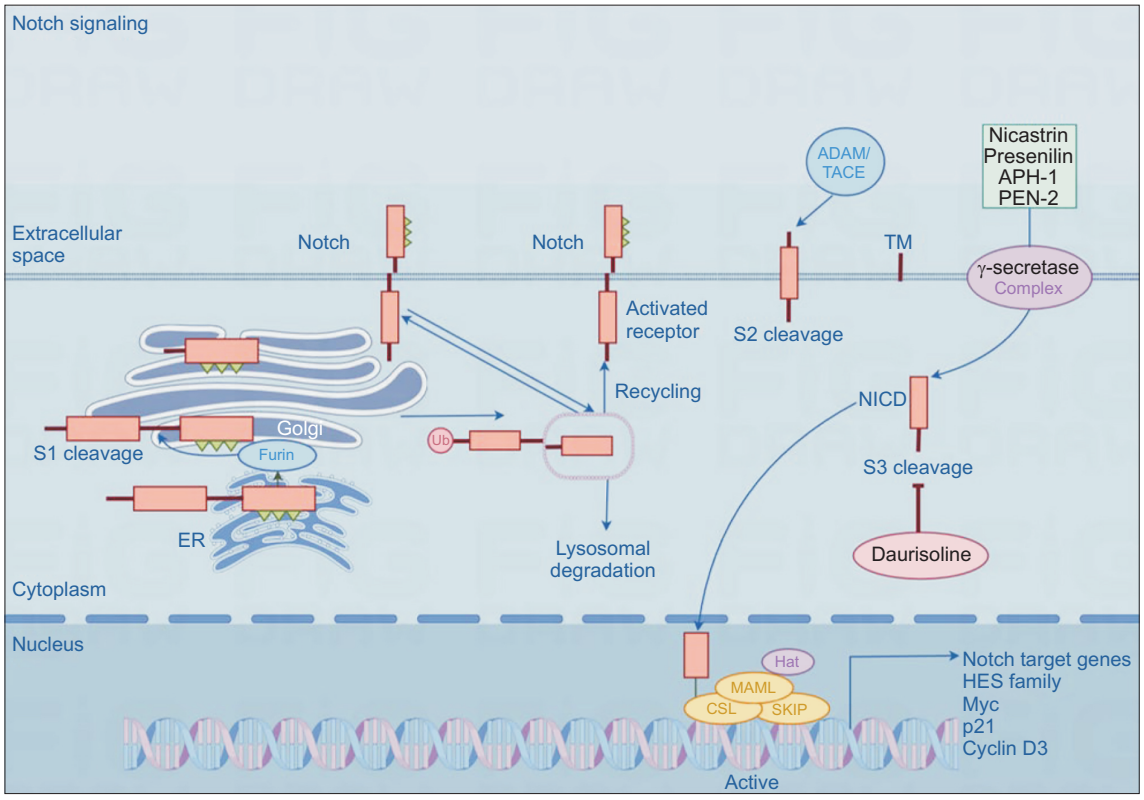

Fig. 8. Diagram of the mechanism of daurisoline against TNBC growth. As a γ-secretase inhibitor, daurisoline reduces the production of NICD by decreasing the hydrolytic activity of γ-secretase on the Notch receptor, which in turn decreases NICD accumulation in the nucleus and its ability to recruit transcription factors. This ultimately prevents the transcription of Notch downstream target genes, thereby affecting the biological behavior of breast cancer cells, including proliferation, migration, and invasion.

γ-secretase inhibitor, suppresses γ-secretase activity, thereby reducing Notch receptor cleavage, decreasing NICD release and nuclear accumulation, and disrupting NICD binding to nuclear transcription factors, such as CSL and MAML. This ultimately inhibits the transcription of downstream Notch target genes, potentially slowing down TNBC progression.

DISCUSSION

The incidence of BC is increasingly observed in younger individuals (Shah *et al*., 2022). Based on the analysis of over 8,000 human genes and corresponding cloned cDNA microarrays, BC is classified into three molecular subtypes: hormone receptor-positive, HER-2-positive, and triple-negative (Ortega-Lozano *et al*., 2022). Among them, TNBC accounts for about 25% of all BC cases and is the most malignant subtype (Calip *et al*., 2022). Natural active ingredients provide a new option for the prevention and treatment of TNBC due to their novel structure, strong specificity, and high safety (Jia *et al*., 2021a).

The abnormal activation of the Notch signaling pathway has exhibited to be associated with the BC progression (Saini *et al*., 2024). The activation of the Notch receptors involves three cleavages, in which the γ-secretase-mediated cleavage is the most critical (Shah *et al*., 2024). The γ-secretase complex, located on the nuclear membrane, cleaves the NECD to release the NICD. NICD can then translocate into the nucleus, bind to transcription factors, such as CSL, MAML, and SKIP, and initiate the transcription of downstream targets, including HES family genes, MYC, P21, and Cyclin D3. In this process, γ-secretase serves as the core target for regulating activation of the Notch signaling pathway.

In this research, it was found that daurisoline derived from RM exhibited anti-TNBC activity. The bisbenzylisoquinoline alkaloids represented by daurisoline showed a strong inhibitory effect on TNBC. Furthermore, it was revealed that the anti-TNBC effects of daurisoline were associated with the γ-secretase/Notch signaling pathway. It was therefore, for the first time, hypothesized that daurisoline, a natural γ-secretase inhibitor, could effectively inhibit the growth of TNBC by blocking the activation of the γ-secretase/Notch axis (Fig. 8).

To validate this hypothesis, two TNBC cell lines, MDA-MB-231 and MDA-MB-468, were selected to assess the anti-TNBC activity of daurisoline. Subsequently, a nude mouse xenograft model was utilized to investigate the anti-tumor effects of daurisoline on TNBC, revealing that daurisoline could effectively inhibit the growth of subcutaneous tumors. To preliminarily clarify whether daurisoline could exert anti-TNBC effects through γ-secretase, molecular docking was employed to simulate the interaction mode between daurisoline and key subunits of γ-secretase. The results indicated that the active functional groups of daurisoline could form intermolecular hydrogen bonds with key amino acid residues of γ-secretase, demonstrating stable binding and notable affinity.

Additionally, the effects of daurisoline on the protein expression levels of the Notch-1 receptor, NICD, and PSEN-1 were assessed, along with the expression levels of apoptosis-related proteins Bax and Bcl-2. This research confirmed that daurisoline could inhibit the proliferation of TNBC cells and promote apoptosis by regulating the γ-secretase/Notch axis, both *in vitro* and *in vivo*.

In conclusion, daurisoline could inhibit the growth of TNBC cells both *in vitro* and *in vivo*. It could induce apoptosis in TNBC cells by regulating the γ-secretase/Notch axis. Daurisoline could decrease the activity of γ-secretase by interfering with the catalytic core PSEN-1, leading to the inhibition of Notch signaling pathway. These results provided valuable insights for further research on daurisoline and Notch signaling pathway, thereby promoting the development of dibenzylisoquinoline alkaloids as targeted therapies for TNBC.

CONFLICT OF INTEREST

All authors declare that there is no conflict of interest.

ACKNOWLEDGMENTS

This study was supported by the National Natural Science Foundation Youth Fund Project (Grant No. 82204685), Natural Science Foundation of Liaoning Province, China (Grant No. 2023-MHLS-286), and basic scientific research projects of colleges and universities of Liaoning Provincial Department of Education (Grant No. LJKMZ20221797).

REFERENCES

Calip, G. S., Nabulsi, N. A., Hubbard, C., Asfaw, A. A., Lee, I., Zhou, J., Cueto, J., Mitra, D., Ko, N. Y., Hoskins, K. F. and Law, E. H. (2022) Impact of time to distant recurrence on breast cancer-specific mortality in hormone receptor-positive breast cancer. *Cancer Causes Control* **33**, 793-799.

Feng, M., Santhanam, R. K., Xing, H., Zhou, M. and Jia, H. (2024) Inhibition of gamma-secretase/Notch pathway as a potential therapy for reversing cancer drug resistance. *Biochem. Pharmacol.* **220**, 115991.

Jia, H., Liu, M., Wang, X., Jiang, Q., Wang, S., Santhanam, R. K., Lv, C., Zhao, Q. and Lu, J. (2021a) Cimigenoside functions as a novel gamma-secretase inhibitor and inhibits the proliferation or metastasis of human breast cancer cells by gamma-secretase/Notch axis. *Pharmacol. Res.* **169**, 105686.

Jia, H., Wang, X., Liu, W., Qin, X., Hu, B., Ma, Q., Lv, C. and Lu, J. (2021b) Cimicifuga dahurica extract inhibits the proliferation, migration and invasion of breast cancer cells MDA-MB-231 and MCF-7 *in vitro* and *in vivo*. *J. Ethnopharmacol.* **277**, 114057.

Jia, H., Wang, Z., Zhang, J. and Feng, F. (2021c) gamma-Secretase inhibitors for breast cancer and hepatocellular carcinoma: from mechanism to treatment. *Life Sci.* **268**, 119007.

Kopan, R. and Ilagan, M. X. (2009) The canonical Notch signaling pathway: unfolding the activation mechanism. *Cell* **137**, 216-233.

Malik, J. A., Ahmed, S., Jan, B., Bender, O., Al Hagbani, T., Alqarni, A. and Anwar, S. (2022) Drugs repurposed: an advanced step towards the treatment of breast cancer and associated challenges. *Biomed. Pharmacother.* **145**, 112375.

Naeem, K., Tariq Al Kury, L., Nasar, F., Alattar, A., Alshaman, R., Shah, F. A., Khan, A. U. and Li, S. (2021) Natural dietary supplement, carvacrol, alleviates LPS-induced oxidative stress, neurodegeneration, and depressive-like behaviors via the Nrf2/HO-1 pathway. *J. Inflamm. Res.* **14**, 1313-1329.

Ortega-Lozano, A. J., Gomez-Caudillo, L., Briones-Herrera, A., Aparicio-Trejo, O. E. and Pedraza-Chaverri, J. (2022) Characterization of mitochondrial proteome and function in luminal A and basal-like breast cancer subtypes reveals alteration in mitochondrial dynamics and bioenergetics relevant to their diagnosis. *Biomolecules* **12**, 379.

Rugo, H. S., Lerebours, F., Ciruelos, E., Drullinsky, P., Ruiz-Borrego, M., Neven, P., Park, Y. H., Prat, A., Bachelot, T., Juric, D., Turner, N., Sophos, N., Zarate, J. P., Arce, C., Shen, Y. M., Turner, S., Kanakamedala, H., Hsu, W. C. and Chia, S. (2021) Alpelisib plus fulvestrant in PIK3CA-mutated, hormone receptor-positive advanced breast cancer after a CDK4/6 inhibitor (BYLieve): one cohort of a phase 2, multicentre, open-label, non-comparative study. *Lancet Oncol.* **22**, 489-498.

Saini, H., Basu, P., Nesari, T., Huddar, V. G., Ray, K., Srivastava, A., Gupta, S., Mehrotra, R. and Tripathi, R. (2024) Therapeutic and pharmacological efficacy of plant-derived bioactive compounds in targeting breast cancer. *Am. J. Transl. Res.* **16**, 1499-1520.

Serneels, L., Narlawar, R., Perez-Benito, L., Municoy, M., Guallar, V., T'Syen, D., Dewilde, M., Bischoff, F., Fraiponts, E., Tresadern, G., Roevens, P. W. M., Gijsen, H. J. M. and De Strooper, B. (2023) Selective inhibitors of the PSEN1-gamma-secretase complex. *J. Biol. Chem.* **299**, 104794.

Shah, A., Haider, G., Abro, N., Bhutto, S., Baqai, T. I., Akhtar, S. and Abbas, K. (2022) Correlation between age and hormone receptor status in women with breast cancer. *Cureus* **14**, e21652.

Shah, H., Mistry, M., Patel, N. and Vora, H. (2024) Erratum to: clinical significance of Notch receptors in triple negative breast cancer. *Breast Dis.* **43**, 159.

Zhou, B., Lin, W., Long, Y., Yang, Y., Zhang, H., Wu, K. and Chu, Q. (2022) Notch signaling pathway: architecture, disease, and therapeutics. *Signal Transduct. Target. Ther.* **7**, 95.